ISIJ International, Vol. 38 (1998), No. 11, pp. 1208–1215

Model Development of Slag Foaming

Surinder S. GHAG, Peter C. HAYES[1)] and Hae-Geon LEE[2)]

RGC Mineral Sands, Capel, WA 6271, Australia. 1) Department of Mining, Minerals and Materials Engineering, The University of Queensland, Brisbane, Qld 4072, Australia. 2) Department of Materials Science and Metallurgical Engineering, Pohang University of Science and Technology, San 31, Hyoja-Dong, Nam-Ku, Pohang, 790-784, Korea.

(*Received on October 31, 1997; accepted in final form on June 22, 1998*)

A general model of foaming has been developed which relates the structure of a foam stabilised by viscoelastic forces to the bubble rupturing processes. For the specific case of negligible bubble coalescence within the foam it has been shown that, in the region of linearity between the foam height and gas flux, the residence time of gas in the foam (Σ) is solely a function of the bubble diameter (d), the liquid phase density (ρ) and viscosity (μ), and the effective elasticity (E_{eff}) resulting from the dynamic adsorption of surface active species:

$$\Sigma = 1 \times 10^6 \left(\frac{\mu \cdot E_{\text{eff}}}{(\rho g)^2 d^3} \right)$$

The model, which shows that the gas bubble diameter has the greatest effect on the retention of gas bubbles within the foam, has been found to be applicable to a range of system in which foams are stabilised by viscoelastic forces.

KEY WORDS: slag; foaming; cold modelling; physical modelling.

1. Introduction

In our companion paper[1)] experimental data was presented on a systematic study of foaming behaviour in water–glycerol solutions. In this paper, a general model of foaming is developed that is applicable to a wide range of systems in which foams are stabilised by viscoelastic forces. Various physicochemical properties of the liquid phase were taken into consideration in developing a model: these include viscosity, surface tension, density, bubble diameter, and surface elasticity.

2. Development of Models

Several different models relating residence time to surface properties, namely, surface tension depression, surface elasticity and effective elasticity have been examined and critically evaluated.

2.1. Model I—Surface Tension Depression

It has been shown[1)] that the residence times of gas bubbles (Σ) in spherical foams are a function of the viscosity (μ), surface tension (σ), and density (ρ) of the liquid phase, the gas bubble diameter (d), and the gravitational constant (g). It is also clear that foams cannot be produced from pure liquids but can be produced on the addition of a surface active agent which lowers the surface tension of the solution relative to the pure liquid. Noting that the surface tensions of different pure liquids differ, it is clear that the stability of foam films is a function of lowering of the solutions surface tension on the addition of the surfactant, the surface tension depression ($\Delta\sigma$), rather than the absolute value of the surface tension. Consequently, any quantitative description of foaming should consider the following variables:

$$\Sigma = f(\rho, g, d, \Delta\sigma, \mu) \quad \text{.....(1)}$$

Using Buckingham's method of dimensional analysis[3)] three dimensionless numbers are obtained from six variables and three fundamental dimensions. The problem can be simplified somewhat if it is considered that the variables (ρg) appear as a single term.[2)] In this case the problem reduces to:

$$\Sigma = f(\rho g, d, \Delta\sigma, \mu) \quad \text{.....(2)}$$

and the analysis results in two dimensional numbers, which are related as follows:

$$\frac{\Sigma \cdot \Delta\sigma}{\mu d} = k \left(\frac{\Delta\sigma}{(\rho g) d^2} \right)^{\delta} \quad \text{.....(3)}$$

Using the experimentally determined data for the spherical foams produced by fine bubbles,[1)] the logarithms of the two dimensionless numbers are plotted in **Fig. 1** together with error bars resulting from uncertainties in the properties.[4)] Linear least square analysis of the data shows the values of the exponent δ and the constant k to be 2.32 and 2.02×10^6 respectively, with a regression coefficient r^2 of 0.926. The explicit relationship between the experimental variables is therefore:

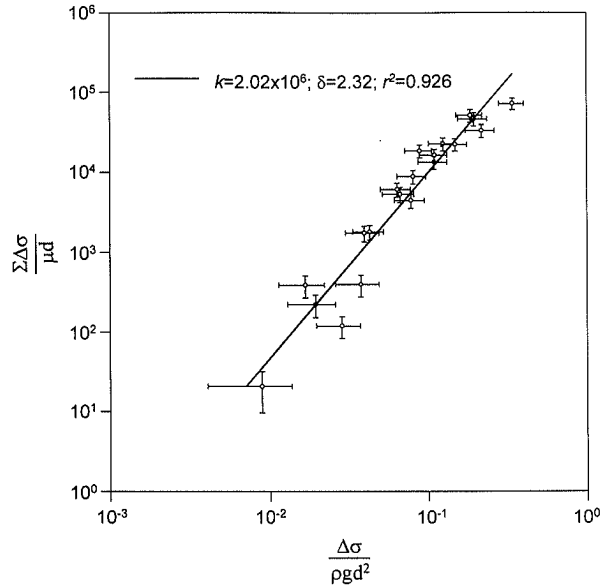

Fig. 1. Dimensional analysis on the raw experimental data obtained from cold modelling experiments[1] using water–glycerol solutions at 20°C.

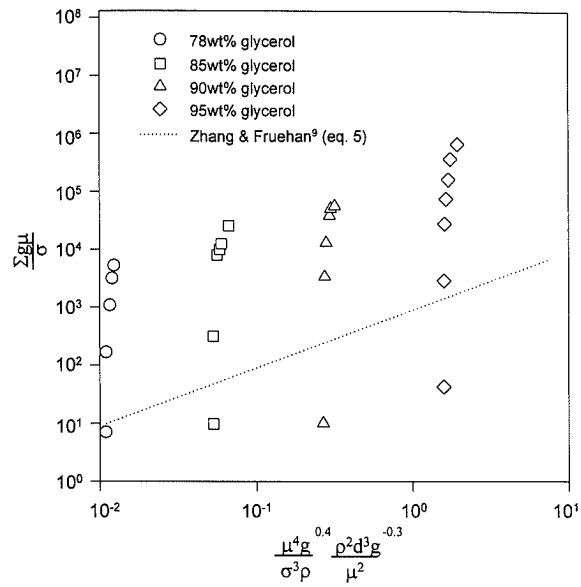

Fig. 2. Comparison of cold modelling experimental data with the relationship derived by Zhang and Fruehan.[9]

Table 1. Calculated properties[5] and gas residence times of $CaO–SiO_2$ slags at 1 873 K.

Basicity	Density (kg/m³)	Viscosity (Pa·s)	Surface tension depression (mN/m)	Bubble diameter (mm)	Gas residence time (s)
0.67	2 545	0.86	219	5	4 798
0.8	2 576	0.55	203	5	2 645
1	2 613	0.35	183	5	1 397
1.35	2 655	0.23	155	5	698

$$\Sigma = 2.02 \times 10^6 \mu \frac{\Delta\sigma^{1.32}}{(\rho g)^{2.32} d^{3.64}} \quad \text{.....(4)}$$

Equation (4) shows that the gas residence times are a linear function of the solution viscosity, and increase non-linearly with increasing surface tension depression, decreasing density and bubble diameter. Clearly, the gas bubble size is the dominant property in determining gas residence times in these spherical foams.

The gas residence times in foams generated from 5 mm diameter bubbles in calcium silicate slags at 1 873 K have been calculated from Eq. (4), with the physico-chemical properties determined from empirical models.[5] The results of these calculations are summarised in **Table 1**. The calculated gas residence times are surprisingly high considering that Cooper and Kitchener found that 5 mm diameter bubbles did not produce a foam in these slags.[6] In the present study it was found that the gas residence time of non-foaming dispersions is of the order of one second.[4]

Various empirical models[7–9] have been developed to describe the relationship between gas residence times and the physico-chemical properties of the slag phase for foams produced by gas injection. The model of Zhang and Fruehan[9]:

$$\Sigma = 115 \frac{\mu^{1.2}}{\sigma^{0.2} \rho d^{0.9}} \quad \text{.....(5)}$$

shows the gas residence times to be directly proportional to the liquid viscosity and inversely related to the mean bubble size. The experimental data obtained from foaming in the water–glycerol–SDBS solutions is plotted in **Fig. 2** in terms of the dimensionless groups used by Zhang and Fruehan. Again, there is a poor correlation between the experimental data and the behaviour predicted by the high temperature model. The major sources of disagreement are due to the exponent of the bubble diameter term and the sensitivity of the gas residence times to changes in the surface tension of the liquid phase. For example, a surface tension depression of 10 mN/m in the cold model system decreases the absolute value of the surface tension by less than twenty percent, but results in up to three orders of magnitude change in the gas residence times.[1] In contrast, Eq. (5) implies that surface forces have only a minimal influence on slag foaming.

Whilst the use of surface tension depression rather than surface tension is beneficial in differentiating between the foaming abilities of different water–glycerol solutions, it is evident that the resultant model is not directly applicable to slag systems which have surface tension depressions more than an order of magnitude higher.

Noting the arguments for similarity in foam stabilisation mechanisms for spherical foams at room temperature and slag foams discussed previously[1] the discrepancies between the above models may result from the use of equilibrium surface tensions or surface tension depressions in the derivation of these models. These assumptions are likely to be in error since foaming is a dynamic, non-equilibrium phenomenon with bubble generation, coalescence and rupture occurring simultaneously.

Clearly to be applicable to a range of systems, the model of foaming must take into direct consideration

the mechanisms of foam stabilisation and their implications. Accordingly, to develop a model for wet, spherical foams that is not system specific, the viscoelastic forces resulting from the adsorption of surface active species are examined and incorporated into the relationship.

2.2. Model II—Surface Elasticity

Consider a thin film produced from a solution consisting of a solvent and a surface active species, in which the bulk solution is initially in equilibrium with the film surfaces. If a section of the film is stretched by some external force, then the instantaneous surface concentration of the surface active species in this stretched region of film will be lower than the equilibrium surface concentration. Therefore the surface tension of the stretched region will be higher than the adjacent unstretched regions, and the surface phase of the stretched region will no longer in equilibrium with the bulk solution. The surface concentration of surfactant in the stretched region can return to equilibrium by one of two mass transfer processes: diffusional mass transfer and adsorption from the underlying bulk solution, or surface flow from the regions of low surface tension to the high surface tension region.

If the relaxation time for diffusion and adsorption is shorter than that for surface flow, then the surface tension gradients generated by stretching are quickly negated by mass transfer from the bulk. However, if the reverse is true, then the surfactant flows from the surfaces of the adjacent unstretched regions of the film to the surfaces of the stretched region as a result of the surface tension gradients produced on deformation. Viscous drag on the underlying bulk solution results in bulk flow accompanying the surface flow. It is this net flow of solution from the thicker sections of the film to the stretched region, resulting from the viscoelastic characteristic of the solution, which provides a mechanism for countering film thinning.[10]

Mathematically, the elasticity of a surface (E) can be expressed as[11]:

$$E=\frac{Ad\sigma}{dA}=\frac{d\sigma}{d\ln A} \quad \text{.....(6)}$$

where A is the surface area, and σ is the surface tension of the solution. Equation (6) shows that the surface elasticity is proportional to the change in surface tension with fractional change in surface area. Cooper and Kitchener[10] propose that any liquid with a positive coefficient of $d\sigma/d\ln A$ should be capable of foaming. Noting that the surface tension depression ($\Delta\sigma$) is equal to the difference in the surface tension of the solvent (σ_0) and solution (σ):

$$\Delta\sigma=\sigma_0-\sigma \quad \text{.....(7)}$$

the elasticity of a single surface can be expressed as[12]:

$$E=-\frac{d\Delta\sigma}{d\ln\Gamma_i}\frac{d\ln\Gamma_i}{d\ln A} \quad \text{.....(8)}$$

where Γ_i is the Gibbs relative surface excess of the surface active species. For a film oscillating at high frequencies such that there is no mass transfer between the surface and the bulk solution, the total quantity of adsorbed surface active species in the surface is constant:

$$\Gamma_i A_s=\text{constant} \quad \text{.....(9)}$$

and the surface behaves as an insoluble monolayer. In this case the elasticity is at a maximum, referred to as the Marangoni dilational modulus. Substitution of Eq. (9) into Eq. (8) results in the following expression for the Marangoni dilational modulus (E_M):

$$E_M=\frac{d\Delta\sigma}{d\ln\Gamma_i} \quad \text{.....(10)}$$

The Marangoni dilational modulus can be readily determined from Eq. (10) once the equation of state for the surface of the system is known. For a system observing ideal, Langmuir behaviour the equation of state is[13]:

$$\Delta\sigma=-RT\Gamma_{i,\infty}\ln\left(1-\frac{\Gamma_i}{\Gamma_{i,\infty}}\right) \quad \text{.....(11)}$$

and for a system following the Frumkin isotherm, which considers attractive interactions between the adsorbed molecules[13]:

$$\Delta\sigma=-RT\Gamma_{i,\infty}\ln\left(1-\frac{\Gamma_i}{\Gamma_{i,\infty}}\right)-a'\left(\frac{\Gamma_i}{\Gamma_{i,\infty}}\right)^2 \quad \text{...(12)}$$

where Γ_i is the Gibbs relative surface excess, $\Gamma_{i,\infty}$ is the Gibbs relative surface excess at saturation of the surface, and a' is related to the enthalpy of adsorption (equal to zero for the Langmuir isotherm). Differentiating Eqs. (11) and (12) in accordance with Eq. (10) results in the following expressions for the Marangoni dilational modulus for the Langmuir:

$$E_M=\frac{RT\Gamma_{i,\infty}\Gamma_i}{(\Gamma_{i,\infty}-\Gamma_i)} \quad \text{.....(13)}$$

and Frumkin isotherms:

$$E_M=\frac{RT\Gamma_{i,\infty}\Gamma_i}{(\Gamma_{i,\infty}-\Gamma_i)}-2a'\left(\frac{\Gamma_i}{\Gamma_{i,\infty}}\right)^2 \quad \text{.....(14)}$$

Using the expressions for the Marangoni dilational modulus given in Eqs. (13) and (14) the relationship between surface tension depressions in water–glycerol–SDBS solutions and the Marangoni dilational moduli are plotted in **Fig. 3**—using values for the parameters $\Gamma_{i,\infty}$ and a' determined previously.[1] It is clear from the figure that the Marangoni dilational modulus increases with increasing surface tension depression. Whilst the Marangoni dilational moduli are similar for all the water–glycerol–SDBS solutions at low surface tension depressions, at higher surface tensions depressions the moduli increase significantly with increasing viscosity of the solutions. These high viscosity solutions obey the Frumkin adsorption isotherm.[1]

It can be seen from Eq. (10) that the dimensions of the Marangoni dilational modulus and the surface tension depression are identical, and, given that the Marangoni dilational modulus represents the maximum elasticity of the film, it is argued that it is appropriate

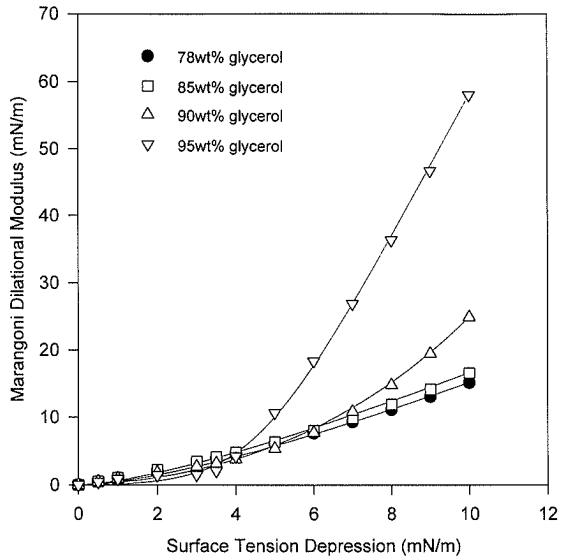

Fig. 3. The Marangoni dilational modulus as a function of surface tension depression for distilled water–AR grade glycerol–SDBS solutions at 20°C.

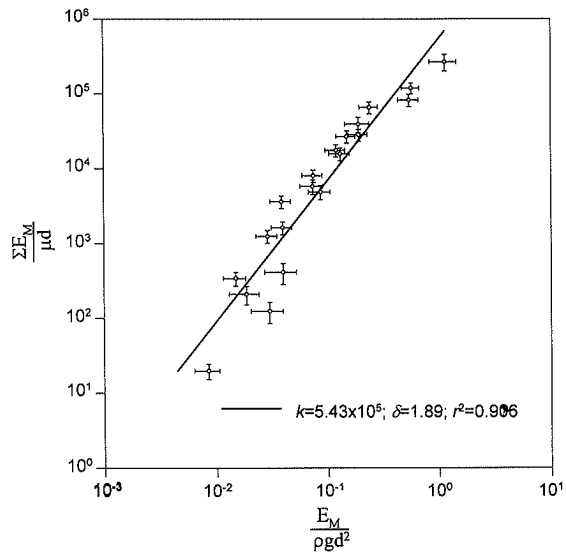

Fig. 4. Dimensional analysis of data obtained from the cold modelling experiments[1] using water–glycerol–SDBS solutions at 20°C. Data analysed in terms of the Marangoni dilational modulus, E_M.

that in the dimensional analysis the Marangoni dilational modulus should be substituted for the surface tension depression *i.e.*

$$f(\Sigma, \rho g, \mu, E_M, d) = 0 \quad \text{.....(15)}$$

The following relationship is obtained between the resulting dimensionless numbers:

$$\frac{\Sigma \cdot E_M}{\mu d} = k\left(\frac{E_M}{(\rho g)d^2}\right)^{\delta} \quad \text{.....(16)}$$

The dimensionless groups in Eq. (16) are plotted in **Fig. 4** using the experimental data obtained for the water–glycerol–SDBS solutions. Least squares regression analysis ($\delta = 1.89$ and $k = 5.43 \times 10^5$) results in the following relationship between the significant system properties:

$$\Sigma = 5.43 \times 10^5 \mu \frac{E_M^{0.89}}{(\rho g)^{1.89} d^{2.78}} \quad \text{.....(17)}$$

However, the regression coefficient of 0.906 for this relationship indicates that the overall fit of the data is in fact poorer than for the analysis in terms of the surface tension depression *i.e.* Eq. (4).

2.3. Model III—Effective Elasticity

In the derivation of Eq. (17) it has been assumed that the elasticity of the bubble films is at its maximum value—the Marangoni dilational modulus. In practice, the effective elasticity can drop below this maximum[14–16] as a result of lower than equilibrium surface concentration of the surfactant prior to film deformation, and reduction of the surface tension gradients generated on deformation by surfactant mass transfer from the bulk solution.

The former process results from insufficient time to attain equilibrium adsorption. The latter results from diffusional mass transfer to the deformed film and is dependent on the frequency of film disturbance—the higher the frequency of disturbance the less time is available for the surfactant to adsorb/desorb from the interface and return the film to a state of equilibrium.

2.3.1. Adsorption Time

The diffusion limited adsorption of a surfactant onto a stationary surface is described by the equation of Ward and Todai.[17] Recently Malysa *et al.*[14,15] have used a numerical solution of this equation[18] to determine the fraction of equilibrium adsorption as a function of time for surfactants obeying Langmuir behaviour. Defining the dimensionless time (Θ) as:

$$\Theta = D t_{ad}\left(\frac{c_i}{\Gamma_i}\right)^2 \quad \text{.....(18)}$$

where D is the diffusivity of the surface active species, t_{ad} is the adsorption time, and c_i is the bulk molar concentration of the surfactant, the solution to the diffusion limited adsorption problem can be expressed in the following polynomial form[18,19]:

$$\frac{\Gamma_i(t_{ad})}{\Gamma_i} = \sum_{i=1}^{N} \xi_i \tau^i \quad \text{.....(19)}$$

where $\Gamma_i(t_{ad})$ is the Gibbs relative surface excess for an adsorption time t_{ad}, and the values of ξ_i are tabulated as a function of the reduced concentration ($c_i/c_{i,L}$) where $c_{i,L}$ is the molar concentration at which $\Gamma_i = 0.5\Gamma_{i,L}$, and τ is defined by:

$$\tau = 1 - \frac{1}{1 + \sqrt{\Theta + \Theta^2 c_i / c_{i,L}}} \quad \text{.....(20)}$$

The maximum elasticity for a specific adsorption time, $E(t_{ad})$, is equal to:

$$E(t_{ad}) = \frac{RT\Gamma_{i,\infty}\Gamma_i(t_{ad})}{(\Gamma_{i,\infty} - \Gamma_i(t_{ad}))} \quad \text{.....(21)}$$

2.3.2. Oscillation Frequency

For a system following Langmuir behaviour, the relationship between the effective elasticity, E_{eff}, and the

maximum elasticity for a specific adsorption time, $E(t_{ad})$ is[14]:

$$E_{eff} = E(t_{ad})\left(1 - \frac{F(w)}{F(0)}\right) \quad \text{.....(22)}$$

where

$$\frac{F(w)}{F(0)} = \frac{\alpha_1(2\alpha_1 + A_1 w)}{\alpha_1^2 + (\alpha_1 + A_1 w)^2} \quad \text{.....(23)}$$

$$\alpha_1 = \left(\frac{w}{2D}\right)^{1/2} \quad \text{.....(24)}$$

$$A_1 = \frac{\Gamma_{i,\infty} c_{i,L}}{D(c_i + c_{i,L})^2} \quad \text{.....(25)}$$

and w is the frequency of bubble oscillation. Equations (22)–(25) show that as the frequency of bubble oscillation increases, the effective elasticity tends to the Marangoni dilational modulus because mass transfer from the bulk to the bubble surface is increasingly inhibited.

2.3.3. Effective Elasticity

The decrease in the effective elasticity $(E(t_{ad})/E_M)$ resulting from the slow diffusion of the surface active species can be determined from Eqs. (18)–(21) by equating the adsorption time (t_{ad}) to the residence time of gas in the system (Σ), as the gas residence time can be considered to be the maximum time available for the adsorption of surface active species onto a non-equilibrium surface. Similarly, the decrease in the effective elasticity resulting from mass transfer at bubble oscillation frequencies below those producing insoluble monolayer behaviour is determined from Eqs. (22)–(25). The results of these calculations for the 85 wt% AR grade glycerol solution are plotted in **Fig. 5**.

Firstly, with regard to the effect of adsorption time (diffusion limited adsorption), the figure shows that for surface tension depressions below 2 mN/m the effective elasticity is markedly smaller than the Marangoni dilational modulus. This indicates that the surface concentration of the surfactant is significantly below the equilibrium value. However, the combination of higher bulk surfactant concentrations and greater residence times[1] with increasing surface tension depression, results in increased mass transfer to the stagnant surfaces, such that the effective elasticity is within 10 % of the Marangoni dilational modulus for surface tension depressions of more than 2 mN/m.

Oscillation frequency shows the opposite trend. While there is negligible mass transfer to the oscillating film surfaces at low surface tension depressions, mass transfer to the bubble surfaces increases significantly with increasing surface tension depression due to the increase in bulk surfactant concentration.[1] This results in a significant decrease in the effective elasticities, especially at low film oscillation frequencies where the resistance to mass transfer of surfactant from the bulk solution to the deforming film surfaces is minimal.

The sum of these two effects results in a shallow maximum in the effective elasticity for surface tension depressions within the range 2–5 mN/m for the 78–85 wt% glycerol solution. Within this range the effective elasticity is approximately within 10 % of the Marangoni dilational modulus.

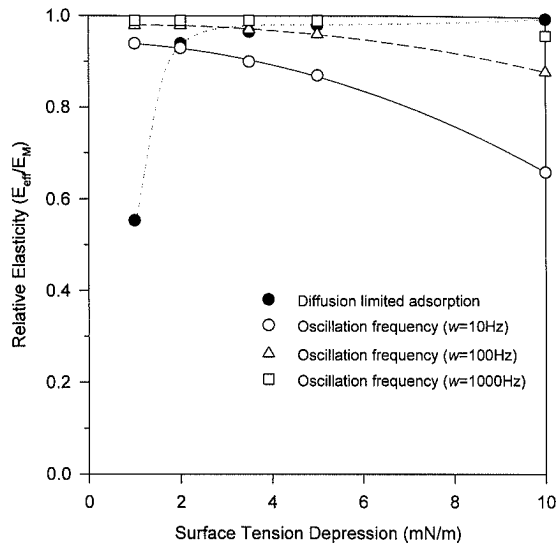

Fig. 5. The effects of diffusion limited adsorption and frequency of film oscillation on the relative elasticity (E_{eff}/E_M) of distilled water–85 wt% AR grade glycerol–SDBS solutions at 20°C.

Whilst the models described above cannot be directly applied to the 90–95 wt% glycerol solutions because they do not follow the Langmuir isotherm, it is argued that it is possible to qualitatively extrapolate the conclusions from the above calculations to these solutions.

Firstly, a combination of higher bulk surfactant concentrations required to generate a specific surface tension depression and higher residence times indicates that the effective elasticity tends to the Marangoni dilational modulus more readily at low surface tension depressions in the 90–95 wt% solutions than the less viscous solutions. The fact that the gas residence times of the 90–95 wt% glycerol solutions are 5–20 times that of the 78–85 wt% solutions[1] for a surface tension depression of 1 mN/m tend to support this argument.

However, it has been shown above that mass transfer to an oscillating surface increases with high bulk surfactant concentrations (especially at low oscillating frequencies), thereby decreasing the effective elasticity. Therefore the effective elasticity of the 90–95 wt% solutions may be expected to decrease significantly as the surface tension depression increases. These predictions are in agreement with the residence time data for high surface tension depressions—whilst Fig. 3 shows that Marangoni dilational modulus for a 95 wt% glycerol solution with a surface tension depression of 10 mN/m is approximately six times that for a 95 wt% glycerol solution with a surface tension depression of 5 mN/m, the gas residence times for the two solutions differ by less than twenty-five percent.[1]

The above analysis shows that the effective elasticity within a system may be significantly lower than the Marangoni dilational modulus over a wide range of surfactant concentrations. It is also evident that the effective elasticities in the water–glycerol–SDBS solutions are within 90–100 % of the Marangoni dilational

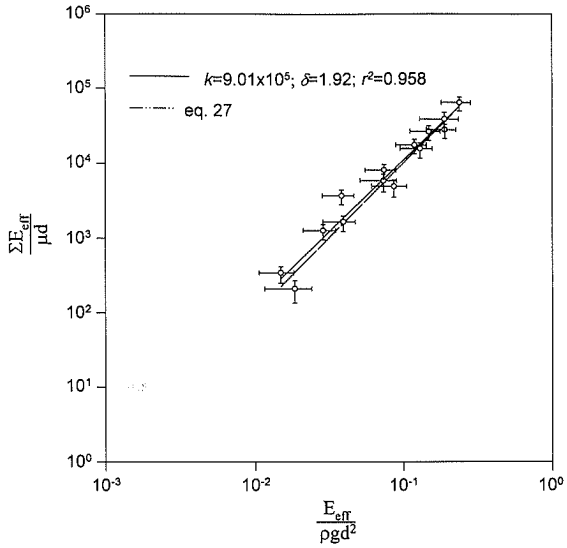

Fig. 6. Dimensional analysis of data obtained from the cold modelling study[1] using water–glycerol–SDBS solutions at 20°C. Analysis conducted using only data with effective elasticities, E_{eff}, within 10 % of the Marangoni dilational modulus.

modulus for surface tension depressions in the range 2–5 mN/m for the 78–85 wt% glycerol solutions and 1–5 mN/m for the 90–95 wt% solutions at all but the lowest oscillation frequencies.

2.3.4. Model Development (Model III)

The data for solutions with effective elasticities within 90–100 % of the Marangoni dilational modulus is plotted in **Fig. 6** in the form:

$$\log\left(\frac{\Sigma \cdot E_{eff}}{\mu d}\right)=\delta \log\left(\frac{E_{eff}}{(\rho g)d^2}\right)+\log k \quad \text{.....(26)}$$

Least squares regression analysis of the data gives $\delta=1.92$ and $k=9.01\times10^5$ with a regression coefficient of 0.958. Taking the uncertainty in the elasticities (resulting from assuming that the effective elasticity is equal to the Marangoni dilational modulus in the range specified above) into consideration the relationship can be simplified to:

$$\left(\frac{\Sigma \cdot E_{eff}}{\mu d}\right)=1\times10^6\left(\frac{E_{eff}}{(\rho g)d^2}\right)^2 \quad \text{.....(27)}$$

with all properties in SI units.

3. Discussion of Model III

3.1. A Physical Interpretation of the Model

Equation (27) can be expressed as:

$$\left(\frac{\Sigma \cdot \rho g d^2}{\mu d}\right)=1\times10^6\left(\frac{E_{eff}}{\rho g d^2}\right) \quad \text{.....(28)}$$

The right-hand side dimensionless number is the ratio of a surface tension related force per unit length and a hydrostatic pressure force per unit length, representing the condition for the rupture of liquid films within the foam—the elastic force counter film rupture while the hydrostatic pressure determines the rate of film drainage.

A physical interpretation of the left-hand side dimensionless number is not so readily apparent. However, if it is assumed that the excess liquid resulting from the rupture of a film drains down the foam through capilaries of radius R and length d, such that, the mean velocity of liquid flow (v) is described by the Haggen–Poiseuille equation for flow resulting from a hydrostatic head, $\rho g d$:

$$v=\frac{\rho g R^2}{8\mu} \quad \text{.....(29)}$$

The capillary drainage time ($\Sigma_{cap}=d/v$) is proportional to:

$$\Sigma_{cap} \propto \frac{\mu d}{\rho g R^2} \quad \text{.....(30)}$$

and under steady-state conditions represents the time required for an underlying film to drain the excess liquid resulting from the rupture of a bubble film without altering the structure of the foam.

The relationship between the film thickness ($2R$), the bubble diameter (d), and the gas fraction (ϕ) for close packed spherical foams is described by the following equation[16]:

$$2R=\left(\frac{1}{\phi}-1\right)\frac{d}{3} \quad \text{.....(31)}$$

Substituting for the capillary radius in Eq. (30):

$$\Sigma_{cap} \propto \frac{\mu d}{\rho g d^2}\left(\frac{1}{\phi}-1\right)^{-2} \quad \text{.....(32)}$$

and substituting Eq. (32) into Eq. (28) results in the following relationship:

$$\left(\frac{\Sigma}{\Sigma_{cap}}\right)\left(\frac{1}{\phi}-1\right)^{-2}=k_1\left(\frac{E_{eff}}{\rho g d^2}\right) \quad \text{.....(33)}$$

Clearly the LHS dimensionless number in Eq. (33) is the product of the ratio of the gas retention (or residence time) and the film drainage time, and a dimensionless number representing the geometry of the foam. Equation (33) shows that the internal dynamics of the foam (in terms of the foam structure, film drainage and gas retention) are determined by the dynamics of bubbles rupture. Therefore the structure of the foam will adjust until at steady-state the drainage ability of the foam matches the rate of bubble rupture. It is this combination of foam structure and the dynamics of bubble rupture that determines the residence times of gas bubbles within the foam.

For spherical foams there is negligible coalescence of bubbles within the foam structure.[20] It is clear from Eq. (33) that under this condition of constant bubble sizes the internal structure of the foam is determined by the rupture of bubbles at the top of the foam. Furthermore, within the regime of linearity between foam height and gas flux, the gas fraction within spherical foams is constant.[20] Therefore the geometry of the foam (Eq. (31)) and consequently capillary drainage of liquid (Eq. (32)) resulting from film rupture at the top of the foam is fixed by the bubble diameter. Under these circumstances, the model can be expressed in the simplified form

shown in Eq. (28) above, or explicitly in terms of the gas residence time:

$$\Sigma = 1 \times 10^6 \left(\frac{\mu \cdot E_{\text{eff}}}{(\rho g)^2 d^3} \right) \quad \text{(s)} \quad \text{.....(34)}$$

Equation (34) shows that the gas bubble diameter has the most significant influence on gas retention within these foams.

3.2. Comparison with Literature Data

Noting the uncertainties in the gas residence times, the relatively large bubble size distributions obtained from the porous disk,[1] and the approximation that the effective elasticities of the distilled water-AR grade glycerol–SDBS solutions are equal to the Marangoni dilational moduli over a significant range of SDBS concentrations, it is necessary to verify the final form of the model for the residence times of gas bubbles in spherical foams (Eq. (34)) with independently determined data. This data was obtained from the studies of Malysa *et al.*[14,15] on foaming in inviscid solutions of n-alkanols and lower fatty acids. These authors determined the residence times of gas in spherical foams generated from these solutions and calculated the effective elasticities resulting from adsorption.

The values of the dimensionless groups:

$$\Pi_1 = \frac{\Sigma \cdot E_{\text{eff}}}{\mu d} \quad \text{.....(35)}$$

$$\Pi_2 = \frac{E_{\text{eff}}}{(\rho g) d^2} \quad \text{.....(36)}$$

have been calculated using the data of Malysa *et al.*,[14,15] considering the viscosities and densities of the solutions to be 1 mPa·s and 1 000 kg/m^3 respectively. Whilst the bubble size was not measured in these studies, the bubble size in a previous investigation using the same apparatus[20] was reported to be in the range 1.3–1.6 mm diameter. Therefore a mean value of 1.45 mm has been used for the purpose of the present calculation.

The results of these calculations have been plotted in **Fig. 7**, which shows that an excellent fit is obtained between the data of Malysa *et al.*[14] for solutions of n-alkanols and the model derived in the present study, and whilst there is a greater scatter in the data for the lower fatty acids,[15] the agreement is still reasonable.

However, it is not surprising that the slope of the data taken from the studies of Malysa *et al.* is approximately equal to 2 when it is noted that these authors assumed a linear relationship between the gas residence times and effective elasticities of the solutions, and then calculated the oscillation frequency to provide the best fit between these two properties.

In contrast, no prior assumption was made in the present study concerning the relationship between these properties. By conducting the analysis in the region where the effective elasticity is within 10 % of the Marangoni dilational modulus, it was possible to determine the relationship between the effective elasticity and the other experimental variables without directly accounting for diffusion phenomena. Consequently, it is clear from Eq.

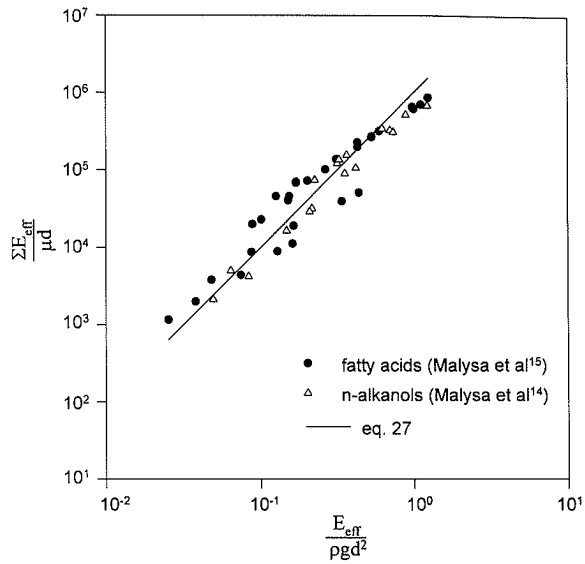

Fig. 7. Comparison of the data of Malysa *et al.* with model derived in the present study–Eq. (27).

(28) and Fig. 7 that present model validates the assumption of Malysa *et al.*[14,15] that the gas residence time is a linear function of the effective elasticity.

Significantly, the comparison of the present model with the data of Malysa *et al.* shows that the data for all these different systems lie on the same line *i.e.* both the exponent, δ, and the constant, k, in Eq. (26) are identical. Therefore the semi-empirical model described by Eq. (28) appears to be valid for a range of systems in which wet, spherical foams are observed.

3.3. Applicability to Metallurgical Slags

The present model for foaming, Eq. (34), considers the effect of the dynamic adsorption of surface active species on foaming, rather than indirectly through the equilibrium surface tension or surface tension depression. The present model applies to spherical foams.

There is no direct evidence available as to whether or not the adsorption of surface active species maintains equilibrium during foaming in metallurgical slag systems. However, the following observations have been reported in the literature, which support the applicability of the present model to foaming of metallurgical slags:

(1) The stability of polyhedral foams decreases with increase in gas velocity.[21]

(2) Quenched slag samples show the spherical nature of slag foams generated by chemical reactions.[22,23]

(3) The thickness of slag film at rupture is observed to be in the range of 10 to 50 μm.[24]

Foams are stabilised either by film elasticity[11] or by the interaction forces in film.[25] If the elasticity of liquid films is sufficient for the films to thin further, film stability is determined by interaction forces acting between adsorbed molecules in this films rather than elastic forces. These interaction forces operate at film thicknesses of less than 100 nm which is of the order of magnitude for films in polyhedral foams.[25] Therefore, the slag film thicknesses of 10 to 50 μm at rupture reported above are far too large for the interaction forces to operate.

The sum of these evidences strongly support that, for

smelting vessels with large diameters and high gas velocities within these systems, slag foams produced are spherical rather than polyhedral in structure and also stabilised by elastic forces. Consequently the present model represented by Eq. (34) can be used for the calculation of gas residence time in slag foams.

4. Conclusions

It has been found that by taking the mechanism of foam stabilisation into direct consideration, a general model can be developed that describes the residence times of gas in spherical foams. The model shows that the internal characteristics of the foam are determined by the bubble rupturing processes. For the specific case of bubbles only rupturing at the top of the foam the gas residence times in the region of linearity between the foam height and gas flux are solely a function of the gas bubble diameter, the liquid phase density and viscosity, and the effective elasticity resulting from the dynamic adsorption of surface active species:

$$\Sigma = 1 \times 10^6 \left(\frac{\mu \cdot E_{\text{eff}}}{(\rho g)^2 d^3} \right) \quad \text{(s)}$$

This model, using SI units, shows that the bubble diameter has the most significant affect on gas retention, with gas retention decreasing with the cube of the bubble diameter.

REFERENCES

1) S. S. Ghag, P. C. Hayes and H.-G. Lee: *ISIJ Int.*, **38** (1998), 1201.
2) J. J. Bikerman: Foams, Springer-Verlag, New York, (1973).
3) E. de St. Q Isaacson and M. de St. Q Isaacson: Dimensional methods in engineering and physics: reference sets and the possibilities of their extension, Edward Arnold, London, (1975).
4) S. S. Ghag: PhD Thesis, Dept. of Mining and Metallurgical Engineering, University of Queensland, Australia, (1996).
5) K. C. Mills and B. J. Keene: *Int. Mater. Rev.*, **32** (1987), 105.
6) C. F. Cooper and J. A. Kitchener: *J. Iron Steel Inst.*, **193** (1959), 48.
7) K. Ito and R. J. Fruehan: *Metall. Trans. B*, **20B** (1989), 509.
8) R. Jiang and R. J. Fruehan: *Metall. Trans. B*, **22B** (1991), 481.
9) Y. Zhang and R. J. Fruehan: *Metall. Mater. Trans. B*, **26B** (1995), 803.
10) C. F. Cooper and J. A. Kitchener: *Q. Rev. Chem. Soc.*, **13** (1959), 71.
11) J. W. Gibbs: The scientific papers of J. Willard Gibbs, Longmans, London, (1906).
12) Q. Jiang and Y. C. Chiew: *Langmuir*, **9** (1992), 273.
13) A. Scheludko: Colloid Chemistry, Elsevier, London, (1966).
14) K. Malysa, K. Lunkenheimer, R. Miller and C. Hempt: *Colloids Surf.*, **16** (1985), 9.
15) K. Malysa, R. Miller and K. Lunkenheimer: *Colloids Surf.*, **53** (1991), 47.
16) K. Malysa: *Adv. Colloid Interface Sci.*, **42** (1992), 37.
17) A. F. H. Ward and L. Todai: Surface Chemistry, Butterworths Scientific Publications, London, (1949).
18) R. Miller and G. Kretzschmar: *Adv. Colloid Interface Sci.*, **37** (1991), 97.
19) R. Miller, P. Joos and V. Fainerman: *Adv. Colloid Interface Sci.*, **49** (1994), 249.
20) R. Cohen, K. Malysa, D. Exerowa and A. Pomianowski: *J. Colloid Interface Sci.*, **80** (1981), 1.
21) S. Hartland and A. D. Barber: *Trans. Inst. Chem. Eng.*, **52** (1974), 43.
22) M. Zamalloa, A. Warczok and T. Utigard: EPD Cong. Min. Met. & Mat. Soc., (1992), 97.
23) S. H. Lee: PhD Theses, Pohang University of Science and Technology, Korea, (1998), 145.
24) C. Nexhip, S. Jahanshahi and S. Sun: 2nd Australian Melt Chem. Symp., GK Williams CRC for Extractive Met., (1995), 111.
25) J. Lyklema: Fundamentals of Interface and Colloidal Science, Vol. 1: Fundamentals, Academic Press, London, (1991).